



Enhanced visible light photocatalytic activity by up-conversion phosphors modified N-doped TiO₂

V. Vaiano*, O. Sacco, G. Iervolino, D. Sannino, P. Ciambelli, R. Liguori, E. Bezzeccheri, A. Rubino

University of Salerno, Department of Industrial Engineering, Via Giovanni Paolo II 132, 84084, Fisciano SA, Italy

ARTICLE INFO

Article history:

Received 3 April 2015

Received in revised form 20 April 2015

Accepted 24 April 2015

Available online 25 April 2015

Keywords:

N-doped TiO₂

Up-conversion organic phosphors

White and green LEDs

Photocatalytic degradation of dyes

ABSTRACT

The development of photocatalytic processes is strongly related to an efficient irradiation of the catalyst surface. A chance to get a significant reactivity enhancement is the promotion of the photocatalyst with up-conversion phosphors able to convert low-energy into high-energy photons. In this work it was found that the photocatalytic activity of visible active N-doped TiO₂ (NdT) can be strongly enhanced when it is promoted by the presence of organic up-conversion phosphors (OP) in the catalyst formulation. Such photocatalysts (NdT/OP) have been prepared and tested in the photocatalytic degradation of a wide range of organic dyes in the presence of visible light irradiation emitted by green or white LEDs. The photocatalytic activity of NdT/OP in the presence of green LEDs is attributed to the up-conversion property of OP phosphors that emit at 434 nm, wavelength suitable for photoexciting NdT. Moreover, NdT/OP showed a dramatic enhancement of photocatalytic activity when white LEDs were used as light source. In this case, the NdT supported on OP surface is excited both by the emission spectrum of the white LEDs and by the blue emission of the phosphors (OP), excited by the green component emitted by white LEDs. The obtained results make NdT/OP photocatalyst a very suitable system to achieve high photocatalytic activity with solar light.

© 2015 Elsevier B.V. All rights reserved.

1. Introduction

The search for a renewable and sustainable energy supply has been intensified in the past years in response to the environmental problems caused by fossil fuels exploitation. In this context, solar energy is clean and very abundant, but its utilization is still very limited. So, it is necessary to develop a sustainable and cost-effective manner for harvesting solar energy to satisfy the growing energy demand of the world with a minimal environmental impact [1].

Photocatalysis can play an important role for the conversion of solar energy into chemicals [2,3], fuels [4,5], electricity [6], and in the removal of organic pollutants both in wastewater [7–9] and in gaseous stream [10].

Since the discovery of the semiconducting properties of TiO₂ (band-gap energy: 3.2 eV) [11], great research efforts have been directed to a better exploitation of solar energy in photocatalysis. However, despite the great number of photocatalyst formulations proposed, most of them are only active under ultraviolet (UV) radiation, which is only a little fraction (5%) of solar light. To be of

practical use for photocatalysis, the photo-response of the transition metal oxides should be within the visible light (43%) of the electromagnetic radiation reaching the planet's surface. Therefore, an appropriate photocatalyst should work in the visible-light region (420 nm < λ < 800 nm) with a band gap of less than 3 eV.

Different approaches to improve the exploitation of sun light in photocatalytic processes have been proposed, especially oxide semiconductors doping [12] or titania photosensitization [13]. However, both approaches still suffer from disadvantages. For example, the introduction of impurities strongly affects the lifetime of the photogenerated e[–]–h⁺ pair, and doping can also decrease the corrosion resistance of the material [14]. Moreover, titania photosensitization with organic dyes still presents major limitations for applications in photocatalysis, due to the poor stability of the dye, which can undergo desorption, photolysis and oxidative degradation, and fast back electron transfer, resulting in low quantum yield for the photocatalytic reaction [15].

Good visible photocatalytic activity results were found on N-doped TiO₂, both under visible irradiation and under solar simulated radiation in the removal of several pollutants such as emerging contaminants [16,17] and bacteria inactivation [18,19]. The photocatalytic performance of a semiconductor material is mainly limited by its intrinsic optical properties as the occurrence

* Corresponding author. Tel.: +39 089 964006; fax: +39 089 964057.

E-mail address: vvaiano@unisa.it (V. Vaiano).

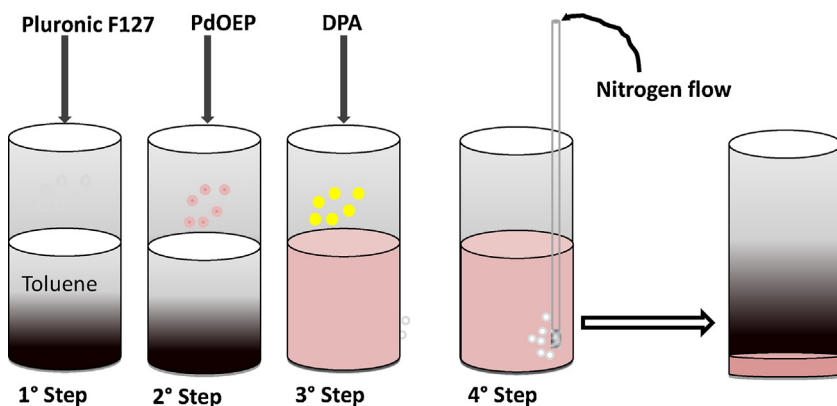


Fig. 1. Schematic picture of OP preparation.

of the photocatalytic reaction requires an excitation source with energy equal or greater than the band gap of the semiconductor [20]. So, a main issue emerged, since the photocatalytic activity is related to the light propagation inside the overall volume of photoreactors [8]. Therefore, since the improving of the photocatalytic reactivity is correlated to an efficient irradiation of the catalytic surface, the chance to get this improvement by modifying a photocatalyst with light carriers such as emitting phosphorescent particles (generally known as phosphors) has been successfully verified to confer additional radiation emission or to decrease the optical path of irradiation towards the photocatalyst [21,22]. A reasonable consequence of such an approach for the intensification of the photocatalytic process seems to be the use of up-conversion phosphors able to convert low-energy into high-energy photons [23]. Few examples report the use of inorganic up-conversion phosphors in a photocatalytic system. To this purpose, active carbon supported undoped TiO_2 catalyst ($\text{C}-\text{TiO}_2$) was modified with $\text{Er}^{3+}:\text{YAlO}_3$ up-conversion phosphors that convert visible light into UV light able to photoexcite TiO_2 [24]. It is worthwhile to highlight that the photocatalytic tests were carried out with a visible light source that is not able to activate undoped TiO_2 .

Moreover, in order to utilize visible light directly, $\text{C}-\text{TiO}_2$ catalyst was modified by blue, green and red colour emitting inorganic up-conversion phosphors through calcination assisted solvothermal method. The characterization data demonstrated that such photocatalysts could be excited by UV, visible and NIR light simultaneously [25]. In this case, all the composites exhibited excellent induced rhodamine B degradation activity under the irradiation of 980 nm NIR laser, although uncoupled phosphors and $\text{C}-\text{TiO}_2$

showed no destruction ability [25]. However, it is very important to underline that only 35% of dye decolourization has been achieved after 5 h of irradiation [25].

Recently, triplet-triplet annihilation up-conversion luminescence has emerged as an efficient process with anti-Stokes shift upon excitation by low power light intensity [26]. When compared to rare-earth up-conversion phosphors, the organic ones have several advantages including more intense absorption coefficient of sensitizer and higher quantum yield [27].

In this work, a visible active N-doped TiO_2 photocatalyst, was modified by organic up conversion phosphors and studied in the photocatalytic degradation of a wide range of organic dyes in the presence of white LEDs visible light irradiation. At our knowledge, it is the first paper reporting the use of organic up-conversion phosphors in a photocatalytic system.

2. Materials and methods

2.1. Materials

Reagents and solvents for the preparation of blue-emissive up conversion organic nanoparticles were: nonionic surfactant Pluronic F127, tetraethyl ortosilicate (TEOS, 99.99%), Pd complex octaethylporphyrin (PdOEP), 9,10-diphenylanthracene (DPA), reagent grade toluene (Aldrich), and hydrochloric acid (fuming, $\geq 37\%$).

Reagents for the synthesis of N-doped TiO_2 catalyst were: titanium(IV) isopropoxide (TTIP, >97 wt%, Sigma-Aldrich) and ammonia aqueous solutions (30 wt%).

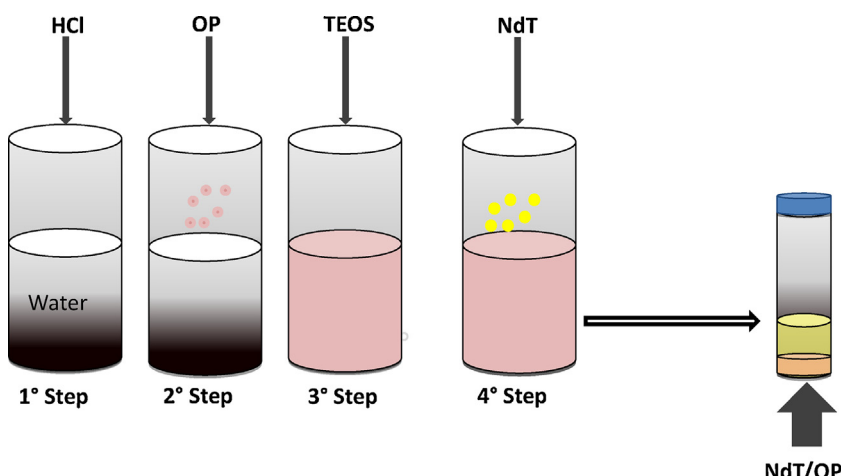


Fig. 2. Schematic picture of NdT/OP preparation.

For the photocatalytic tests, methylene blue (MB), crystal violet (CV), eriochrome black-T (EBT), Rhodamine B (RhB), red allura (RED) and tartrazine (TRZ) (Aldrich) were used.

2.2. N-doped TiO_2 preparation

N-doped TiO_2 (NdT) was prepared by hydrolysis reaction between titanium tetraisopropoxide and 30 wt% ammonia aqueous solution [9]. The preparation was carried out at 0 °C and under stirring until the formation of a gel. The obtained gel was centrifuged and washed with distilled water and then placed in a furnace at 450 °C for 30 min. The molar ratio N/Ti is 18.6, the same as in the catalyst formulation optimised in a previous work [18,28]. The characterization of NdT catalyst, yellow in colour, by different analytical techniques has been reported in our previous papers [18,28]. In particular, UV-vis spectra evidenced the ability of NdT to absorb visible light, as shown by the band gap value (2.5 eV) [28].

2.3. Blue-emissive up-conversion organic nanoparticles preparation

Blue-emissive up-conversion organic nanoparticles (OP) (with a size ranging between 10 and 22 nm [26] were prepared following the method reported by Liu et al. [26]. In particular, 2.0 g of Pluronic F127, 1.0 mg of PdOEP, and 10 mg of DPA were carefully solubilised in 20 mL of toluene. Toluene was evaporated from the homogeneous organic solution by means of a gently nitrogen flow until to obtain a pink solid residue (OP). The schematic picture of the preparation procedure is reported in Fig. 1.

2.4. Preparation of NdT/OP catalyst

OP nanoparticles (0.4 g) were dissolved under magnetic stirring in 25 mL of HCl (0.85 mol L⁻¹) aqueous solution. First TEOS (2 mL), and then NdT (0.12 g) were added to the solution (Fig 2). The mixture was kept under stirring for 48 h at 25 °C and then centrifuged to recover the final NdT/OP solid phasee. The nominal loading of NdT in the catalyst was 30 wt% [29].

2.5. Samples characterization

The samples were characterized with several techniques. Specific surface area of catalysts were obtained by N_2 adsorption measurement at -196 °C with a Costech Sorptometer 1040 after pretreatment at 60 °C for 120 min in He flow (99.9990%). UV-vis reflectance spectra were recorded with a PerkinElmer spectrometer Lambda 35. The TiO_2 content of the NdT/OP sample was determined by X-ray fluorescence spectrometry (XRF) in a thermoFischer ARL QUANT'X EDXRF spectrometer equipped with a rhodium standard tube as the source of radiation and with Si-Li drifted crystal detector. X-ray diffraction (XRD) was carried out using an X-ray microdiffractometer Rigaku D-max-RAPID (Cu-K α radiation). Raman spectra were obtained at room temperature with a Dispersive MicroRaman spectrophotometer (Invia, Renishaw), equipped with a 514 nm diode-laser, in the range 100–2500 cm⁻¹.

For the evaluation of photoluminescence spectrum (PL) of OP nanoparticles, a suspension in distilled water was prepared in a magnetically-stirred cuvette. The sample was irradiated with a 150 W Xe lamp and the excitation wavelength was selected by the use of a LOT MSH-150 monochromator system. The excitation light was guided through a focusing lens and PL was detected by a SM442CCD spectrometer placed at 45° to the incident light beam.

2.6. Photocatalytic activity test

Photocatalytic experiments were carried out with a pyrex tubular photoreactor (internal diameter = 2.5 cm) equipped with an air

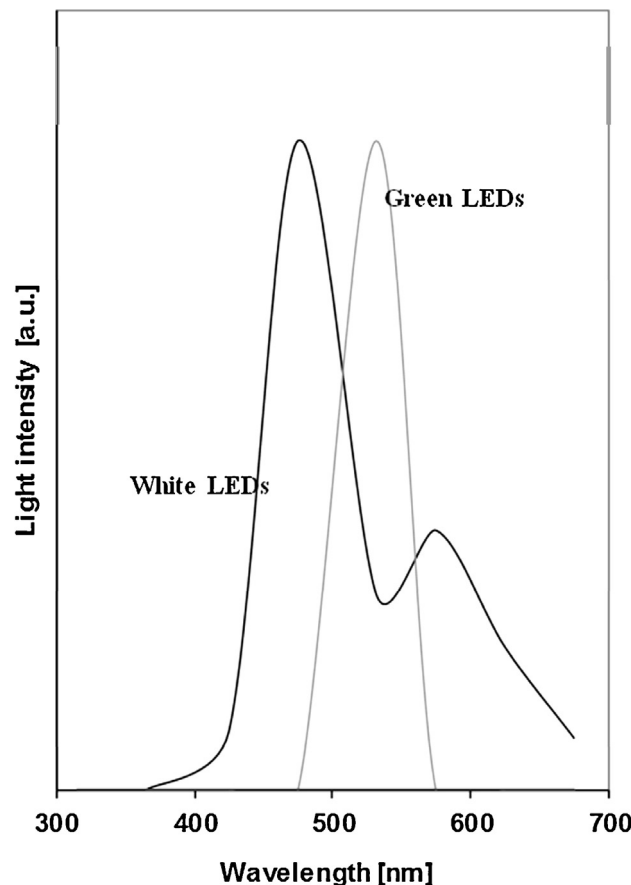


Fig. 3. Emission spectrum of the Green and White LEDs sources.

distributor device ($Q_{air} = 150$ mL/min (STP)), a magnetic stirrer to maintain the photocatalyst suspended in the aqueous solution and a temperature controller [16]. The photoreactor was irradiated by a strip composed of 30 white light LEDs (nominal power: 6W) with wavelength emission in the range 400–800 nm or by the same number green light LEDs (nominal power: 6W) with wavelength emission in the range 450–600 nm (with a maximum centered at about 532 nm) (Fig. 3). The LEDs strip was positioned around the reactor to assure uniform illumination of the reaction volume.

In a typical photocatalytic test, 3 g/L of photocatalyst was suspended in 50 mL solution. The system was kept in dark condition for 2 h to reach dye adsorption equilibrium on the catalyst surface, and then the photocatalytic reaction was initiated by the LEDs lighting. Liquid samples were taken at regular time intervals during the test and centrifuged for 20 min at 4000 rpm for removing the photocatalyst particles. The centrifuged samples were analysed to determine the change of dye concentration, measured with a PerkinElmer UV-vis spectrophotometer at $\lambda = 663, 528, 426, 506, 583$ and 553 for MB, EBT, TRZ, RED, CV and RhB, respectively. The initial concentration of dyes in the photocatalytic tests was equal to 10 mg/L.

3. Results and discussion

3.1. Characterization of the samples

All the catalysts are listed in Table 1, together with nominal and measured NdT loading, specific surface area (BET), equivalent band-gap energy, and NdT average crystallites size.

The specific surface area (SSA) of pure NdT, after calcination in air at 450 °C, is 30 m²/g, while a lower value (1 m²/g) was found

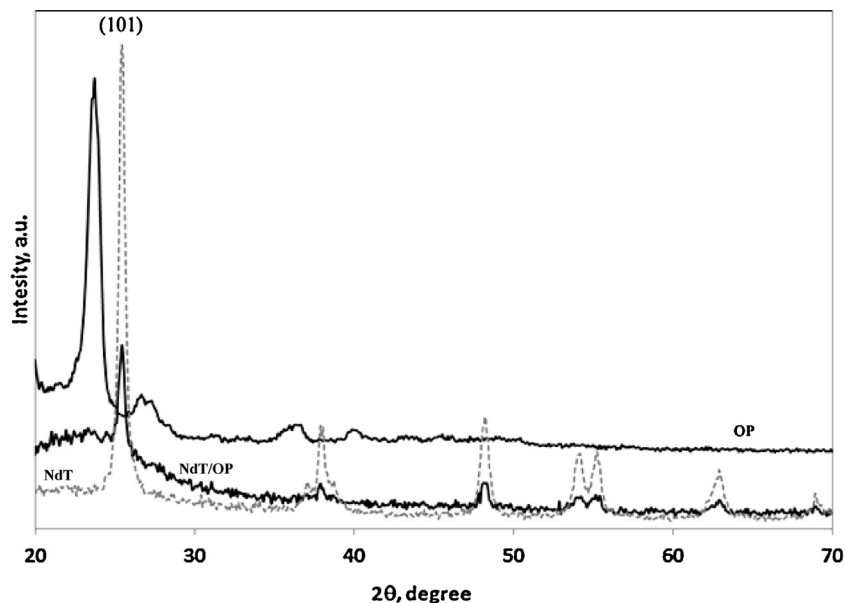


Fig. 4. XRD analysis of NdT, OP and NdT/OP.

for OP. It is worthwhile to note that the SSA of NdT/OP catalyst increased up to $8\text{ m}^2/\text{g}$ after the deposition of NdT on the surface. The increase of surface area could be ascribed to the formation of NdT coating on the OP surface.

The total amount of titania in NdT/OP catalyst, determined by XRF, well agrees with the nominal TiO_2 amount, indicating that the preparation method is a suitable way to couple NdT with OP phosphors.

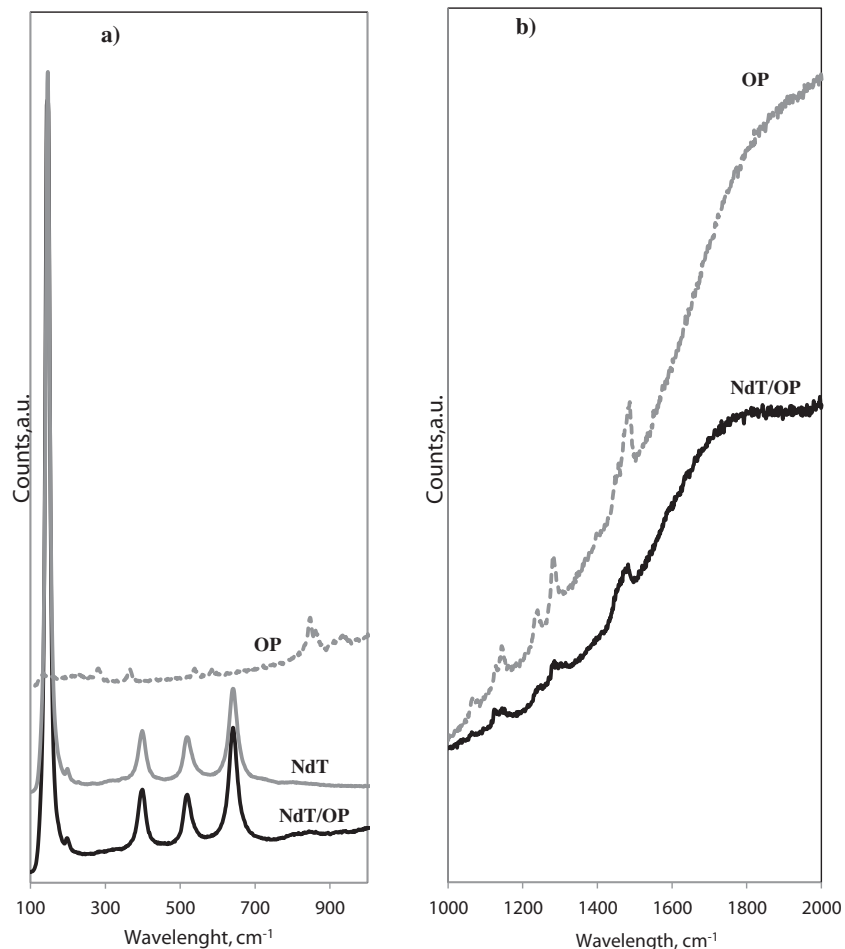


Fig. 5. Raman spectra of the samples OP, NdT and NdT/OP in the range: (a) $100\text{--}1000\text{ cm}^{-1}$ and (b) $1000\text{--}2000\text{ cm}^{-1}$.

Table 1

List of the catalysts and their characteristics.

Sample	TiO ₂ nominal loading wt/%	TiO ₂ measured loading (XRF) wt/%	Specific surface area m ² /g	TiO ₂ average crystallites size nm	Equivalent Band gap energy eV
NdT	100	100	30	17	2.5
OP	–	–	1	–	–
NdT/OP	30	28	8	17	–

Crystal phase composition and crystallinity of the materials were determined by XRD (Fig. 4). Anatase was the only TiO₂ crystalline phase detected for both NdT and NdT/OP. This result suggests that the preparation method used for obtaining the catalyst did not induce any change in the NdT crystalline structure, as also evidenced by the same value of crystallite size, evaluated at diffraction plane (1 0 1) through the Scherrer equation (Table 1). In the case of NdT/OP, a broad band with low intensity centred at $2\theta = 23^\circ$ appears, attributed to silica obtained from the hydrolysis of TEOS [30]. The main diffraction signals of OP disappeared in NdT/OP pattern, due to the covering of OP surface by silica and NdT.

Raman spectra of NdT, OP and NdT/OP are shown in Fig. 5. In the range 100–1000 cm⁻¹ (Fig. 5a), NdT showed bands at 144, 396, 514, 637 cm⁻¹ and a weak shoulder at 195 cm⁻¹, due to the Raman-active fundamental modes of anatase [31].

The NdT/OP catalyst also shows the presence of some bands of NdT without any shift in their positions. This indicates that the dispersion of NdT on the OP surface did not cause modification in the crystalline structure of NdT catalyst, as shown by XRD analysis.

In the range 100–1000 cm⁻¹, the spectrum of OP displayed signals at 281, 366, 536, 582, 847 and 926 cm⁻¹, less intensive than those ones of NdT. These signals disappear when NdT is supported on the surface of OP. On the contrary, in the range 1000–2000 cm⁻¹ (Fig. 5b), the OP spectrum displayed signals at 1065, 1146, 1233, 1280, 1455 and 1486 cm⁻¹, that are present also in NdT/OP, but with lower intensity (Fig. 5b).

Fig. 6 depicts the PL spectrum of OP excited at 532 nm wavelength, accordingly with the spectral distribution of green LEDs employed to irradiate the photoreactor. A wide emission band between 400 and 500 nm was detected, with a blue peak centred at about 434 nm and two blunter peaks located at 418 and 450 nm, in good agreement with the data previously published [26].

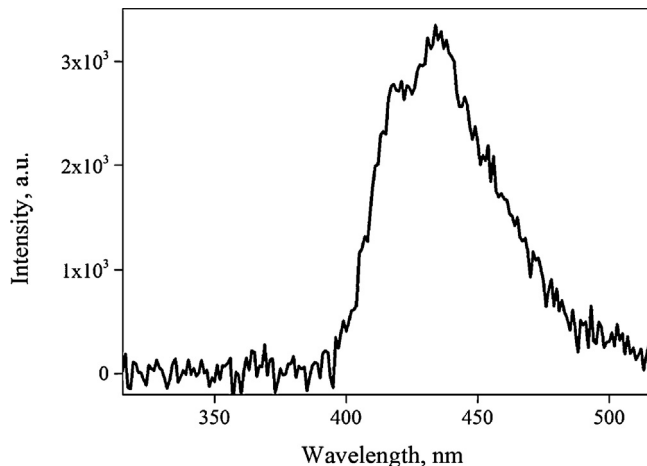


Fig. 6. Photoluminescence spectrum of OP sample excited by a 532 nm source.

3.2. Photocatalytic activity tests with green LEDs as light source

To understand the influence of OP blue emission on NdT photoactivity, a photocatalytic test was carried out with MB dye solution (initial concentration of 10 mg/L) and green LEDs as light source. As reported in the Fig. 7 (insert), photocatalytic test on NdT showed that the MB concentration reached a maximum value, likely due to MB desorption from the NdT surface, and then decreased. After 240 min of irradiation, the MB degradation reached a value of about 3% indicating that NdT has only a negligible photoactivity in the presence of green LEDs. It is worthwhile to consider

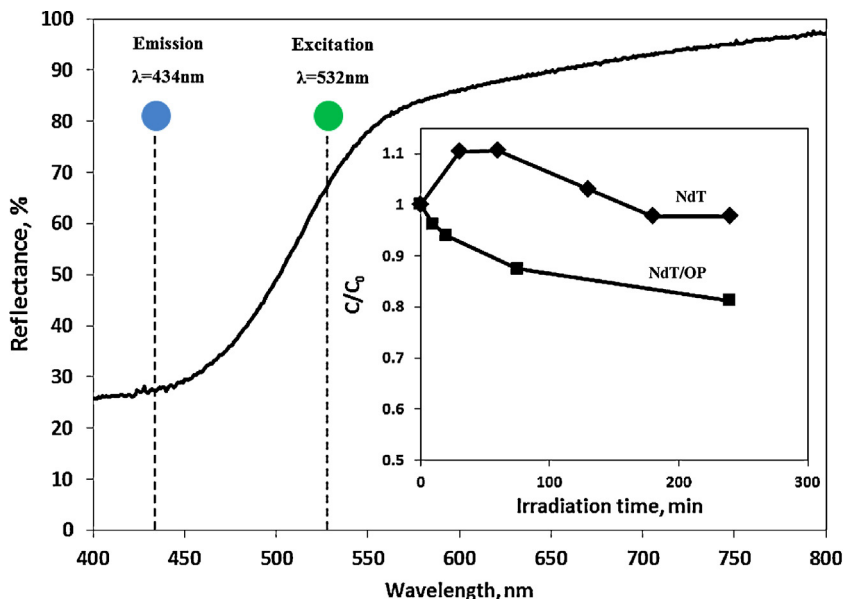


Fig. 7. Reflectance spectrum of NdT sample and behavior of MB concentration as a function of irradiation time on NdT and NdT/OP composite (insert); light source: green LEDs.

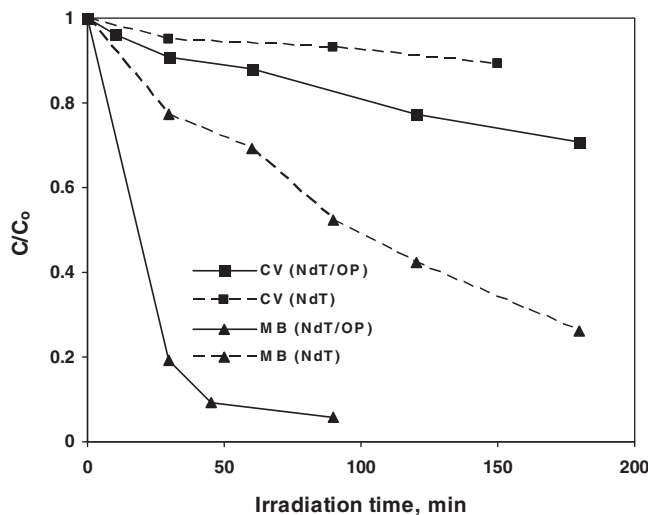


Fig. 8. Photocatalytic decolourization of MB and CV on NdT and NdT/OP; light source: white LEDs.

that at these operating conditions no photolysis of MB occurred (not shown).

A dramatically different trend was found for the NdT/OP catalyst, which showed MB degradation of about 20% after 4 h of irradiation. These results clearly indicate that the photocatalytic activity under green light is only due to the presence of OP, that has up-conversion property and emits at 434 nm, wavelength able to photoexcite the N-doped titania deposited on OP surface, as also confirmed by the UV-vis DRS spectrum of NdT (Fig. 7). Indeed, the NdT catalyst evidenced a reflectance value of about 27% at excitation wavelength of 434 nm, corresponding to the blue emission of OP. On the contrary, with excitation wavelength of 532 nm (corresponding to the maximum emission of green LEDs), the NdT catalyst showed a very higher reflectance value with respect to that one at 434 nm. In summary, when NdT/OP is excited at 532 nm with green LEDs, OP nanoparticles emit at 434 nm, subsequently, the up-converted visible photons were absorbed by NdT leading to a better efficiency in MB photocatalytic degradation than NdT photocatalyst following a mechanism similar to that one found by Zhang et al. [32].

3.3. Photocatalytic activity tests with white LEDs as light source

In order to verify that the dyes were converted in a heterogeneous photocatalytic process, blank experiments were performed. In particular, tests carried out in dark conditions with all the investigated dyes did not evidence any oxidation activity. Moreover, additional control tests were carried out in the presence of each dye and irradiating the photoreactor with white LEDs (photolysis reaction) and in the absence of photocatalyst. Also in this case, no degradation of the target dye was detected.

The results of photocatalytic activity testing with NdT and NdT/OP for MB, CV, RhB, EBT, TRZ and RED are reported in Figs. 8–10. For all the dyes a very strong increase of photocatalytic activity was found with NdT/OP with respect to NdT.

In particular, Fig. 8 gives a clear evidence of the dramatic enhancement of the photocatalytic decolourization rate of MB due to the presence of OP; NdT/OP allows to obtain 80% MB degradation after only 30 min of irradiation time, while with the NdT only 30% degradation was achieved after the same irradiation time.

Moreover, while the photocatalyst NdT did not allow to reach an effective degradation of CV dye, the NdT/OP catalyst improved the efficiency of the process reaching 30% degradation after 180 min of irradiation, much higher than that obtained with NdT (about 11%).

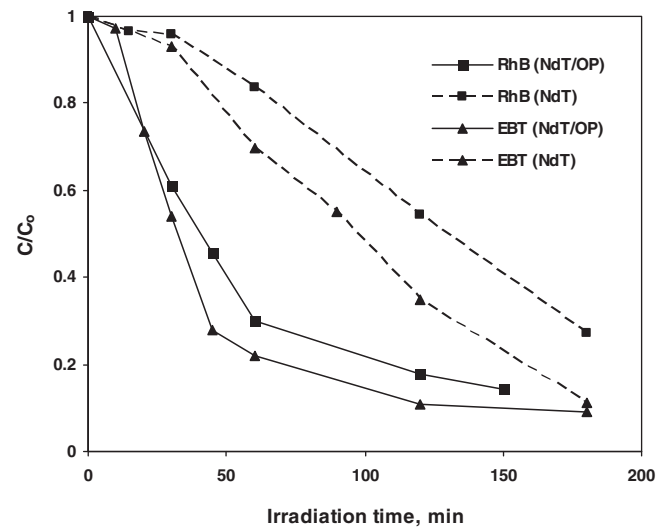


Fig. 9. Photocatalytic decolourization of RhB and EBT on NdT and NdT/OP; light source: white LEDs.

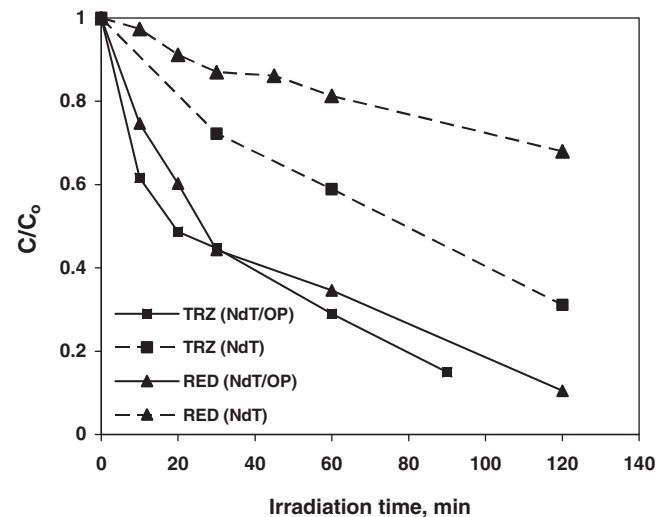


Fig. 10. Photocatalytic decolourization of TRZ and RED on NdT and NdT/OP; light source: white LEDs.

after the same irradiation time. The same trend was found for RhB, EBT, TRZ and RED dyes (Figs. 9 and 10).

The dramatic enhancement of photocatalytic activity obtained in this work is related to the specific formulation of the NdT/OP photocatalyst. It is possible to retain that NdT supported on the OP surface is excited both by the blue component of the emission spectrum of the white LEDs, and by the blue emission of the phosphors (OP), excited in turn by the green component emitted by the white LEDs. This phenomenon contributes to strongly enhance the NdT/OP photoactivity when it is irradiated with white LEDs.

4. Conclusions

In this work we have found that the photocatalytic activity of visible active N-doped TiO_2 (NdT) can be strongly enhanced when it is promoted by the presence of organic up-conversion phosphors (OP) in the catalyst formulation. A wide range of organic dyes was photocatalytically degraded in the presence of visible light irradiation emitted by green or white LEDs. It is possible to retain that the photocatalytic activity of N-doped TiO_2 supported on up-conversion phosphors (NdT/OP) under green light is due to the presence of the

phosphors, that has up-conversion property and emits at 434 nm, wavelength able to photoexcite the NdT deposited on the OP surface. The NdT/OP catalyst shows high photocatalytic activity when white LEDs are used as light source. In this case, the NdT supported on the OP surface is excited both by the blue component of the emission spectrum of the white LEDs, and by the blue emission of the phosphors (OP), excited by the green component emitted by white LEDs. This phenomenon contributes to strongly enhance the photocatalytic activity of NdT/OP photocatalyst in the decolorization process of all the tested dyes.

The obtained results make the visible active NdT photocatalyst modified with organic up-conversion phosphors, a very suitable system to achieve high photocatalytic activity with solar light.

Acknowledgement

The authors wish to thank “POR Campania Rete di Eccellenza FSE. Progetto “Tecnologie e monitoraggio ambientale per la sostenibilità delle Aree Vaste” (TEMASAV), CUP B25B09000090009”.

References

- [1] H. Chen, L. Wang, *Beilstein J. Nanotechnol.* 5 (2014) 696–710.
- [2] C. Guarisco, G. Palmisano, G. Calogero, R. Ciriminna, G. Di Marco, V. Loddo, M. Pagliaro, F. Parrino, *Environ. Sci. Pollut. Res.* 21 (2014) 11135–11141.
- [3] G. Palmisano, *Curr. Org. Chem.* 17 (2013) 2365.
- [4] G.L. Chiarello, M.V. Dozzi, M. Scavini, J.D. Grunwaldt, E. Sell, *Appl. Catal. B: Environ.* 160–161 (2014) 144–151.
- [5] G.L. Chiarello, D. Ferri, E. Sell, *J. Catal.* 280 (2011) 168–177.
- [6] M. Antoniadou, V. Vaiano, D. Sannino, P. Lianos, *Chem. Eng. J.* 224 (2013) 144–148.
- [7] V. Vaiano, O. Sacco, D. Sannino, P. Ciambelli, *Appl. Catal. B: Environ.* 170–171 (2015) 153–161.
- [8] V. Vaiano, O. Sacco, M. Stoller, A. Chianese, P. Ciambelli, D. Sannino, *Int. J. Chem. Reactor Eng.* 12 (2014) 1–13.
- [9] V. Vaiano, O. Sacco, D. Sannino, P. Ciambelli, S. Longo, V. Venditto, G. Guerra, *J. Chem. Technol. Biotechnol.* 89 (2014) 1175–1181.
- [10] M. Hajaghazadeh, V. Vaiano, D. Sannino, H. Kakooei, R. Sotudeh-Gharebagh, P. Ciambelli, *Catal. Today* 230 (2014) 79–84.
- [11] A. Fujishima, X. Zhang, *Comptes Rendus Chimie* 9 (2006) 750–760.
- [12] S.U.M. Khan, M. Al-Shahry, W.B. Ingler, Jr. *Sci. (Washington DC, U.S.)* 297 (2002) 2243–2245.
- [13] J. Zhao, C. Chen, W. Ma, *Top. Catal.* 35 (2005) 269–278.
- [14] H. Kisch, W. Macyk, *ChemPhysChem* 3 (2002) 399–400.
- [15] Y. Zhao, J.R. Swierk, J.D. Megiatt, B. Sherman Jr., W.J. Youngblood, D. Qin, D.M. Lentz, A.L. Moore, T.A. Moore, D. Gust, T.E. Mallouk, *Proc. Natl. Acad. Sci. U. S. A.* 109 (2012) S15612–S15618.
- [16] V. Vaiano, O. Sacco, D. Sannino, P. Ciambelli, *Chem. Eng. J.* 261 (2015) 3–8.
- [17] J. Senthilnathan, L. Philip, *Chem. Eng. J. (Amsterdam Neth.)* 172 (2011) 678–688.
- [18] L. Rizzo, D. Sannino, V. Vaiano, O. Sacco, A. Scarpa, D. Pietrogiacomi, *Appl. Catal. B: Environ.* 144 (2013) 369–378.
- [19] Y. Liu, J. Li, X. Qiu, C. Burda, *J. Photochem. Photobiol. A* 190 (2007) 94–100.
- [20] W. Yang, X. Li, D.H. Chi Zhang, X. Liu, *Nanotechnology* 25 (2014) 482001–482016.
- [21] P. Ciambelli, D. Sannino, V. Palma, V. Vaiano, R.S. Mazzei, *Photochem. Photobiol. Sci.* 10 (2011) 414–418.
- [22] X. Wu, S. Yin, Q. Dong, B. Liu, Y. Wang, T. Sekino, S.W. Lee, T. Sato, *Sci. Rep.* 3 (2013) 2918.
- [23] F. Wang, X. Liu, *Chem. Soc. Rev.* 38 (2009) 976–989.
- [24] S. Dong, X. Zhang, F. He, S. Dong, D. Zhou, B. Wang, *J. Chem. Technol. Biotechnol.* 90 (2015) 880–887.
- [25] X. Wu, S. Yin, Q. Dong, T. Sato, *Appl. Catal. B* 156–157 (2014) 257–264.
- [26] Q. Liu, T. Yang, W. Feng, F. Li, *J. Am. Chem. Soc.* 134 (2012) 5390–5397.
- [27] T.N. Singh-Rachford, F.N. Castellano, *Coord. Chem. Rev.* 254 (2010) 2560–2573.
- [28] O. Sacco, M. Stoller, V. Vaiano, P. Ciambelli, A. Chianese, D. Sannino, *Int. J. Photoenergy* 2012 (2012).
- [29] O. Sacco, V. Vaiano, C. Han, D. Sannino, D.D. Dionysiou, *Appl. Catal. B: Environ.* 164 (2015) 462–474.
- [30] Y. Yusof, M.R. Johan, *CrystEngComm* 16 (2014) 8570–8575.
- [31] P. Ciambelli, D. Sannino, V. Palma, V. Vaiano, R.L. Bickley, *Appl. Catal. A: Gen.* 349 (2008) 140–147.
- [32] M. Zhang, Y. Lin, T.J. Mullen, W.-F. Lin, L.-D. Sun, C.-H. Yan, T.E. Patten, D. Wang, G.-Y. Liu, *J. Phys. Chem. Lett.* 3 (2012) 3188–3192.